Analysis of Lidar's ability in wetland investigation -a case study in Yellow River Delta

Qiong Ding*, Wu Chen, Bruce King

Department of Land Surveying and Geo-Informatics, Hong Kong Polytechnic University, Hong Kong-08902630R@polyu.edu.hk

Abstract: This study assesses the contribution of LIDAR altimetry, multi-return and intensity information, and aerial photos to coastal wetland investigation. Aerial photos in this area work as reference data to assess the accuracy of the experiment. The performance of Lidar data resources was tested alone with the adaptive TIN algorithms to separate ground points. Multi-return information was employed to conduct vegetation extraction as Lidar can penetrate canopy and reach the ground. Intensity is also used to assist classification due to its variability on different objects. The result demonstrated that LIDAR can work as a fast and robust mean for detailed mapping of coastal wetland underlying terrain, investigation of the vegetation, and exploration of coastal area with different moisture. It provides more reliability in wetland mapping and classification compared with remote sensing images alone.

Key words: LiDAR, coastal wetland, multi-return, intensity, classification.

1. INTRODUCTION

The Yellow River is the birthplace of ancient Chinese culture and the cradle of Chinese Civilization. Due to the great amount of sand and mud deposited, the well-known Yellow River Delta (YRD) region was formed during the past thousands of years and it is still extending to the sea continuously. YRD owns the youngest, vastest and most complete wetlands ecosystem of warm temperate zone in the world. It also offers a wonderful place for transferring, wintering and inhabiting for many birds from northeast of Asian and west of Pacific Ocean. The YR wetland is more complicated than inland wetland, because it is affected by the sea, river and land simultaneously. YRD region is an ecologically and physically diverse place and provides a natural laboratory for researches in different disciplines. Ecologists take this area as a base to study the form, evolvement and development of newly created land; biologists take it as a gene pool to research the law for organism derivation and succession; climate protectors take it as a mirror to reflect the improving results of the YR.

To protect the fragile ecosystem and prevent further loss of wetland, many researchers paid attention to inventorying and monitoring wetlands. Satellite remote sensing is a commonly used method. Satellite images for the same area can be collected repeatedly so that wetlands can be monitored seasonally or yearly. It is also less cost and time-consuming in land cover classification than using aerial photography for large geographic areas. In some early work, Yue (2003) conducted supervised classification by integrating Landsat TM images of the newly created wetland in the YRD in the four seasons of each year to detect the landscape change. Xu (2003) studied the characteristics of wetland landscape changes by the remote sensing images acquired in 1976, 1986 and 1996 separately. Li (2007) combined remote sensing and Geographic Information System technology to study the YR wetland changes. However, limitations are existed for ecological applications in conventional sensors. The sensitivity and accuracy of the sensors can't produce accuracy estimation of aboveground biomass and leaf area index (Waring et al. 1995, Carlson et al. 1997, Turner et al. 1999). The resolution of satellite images is too coarse to extract detail information. They are also limited in their ability to represent the spatial patterns. However, LiDAR can directly measure the distance between the targets and platform. It provides 3D information on the target, which enables the estimation of many ecological variables, such as canopy height, above ground biomass. The purpose of this study is to assess the contribution of LIDAR altimetry, multi-return and intensity information, and aerial photos to coastal wetland investigation.

2. STUDY SITE

2.1 Study site description

Due to the huge dataset of the whole area, two blocks of the YRD wetland with size of 750m*750m were chosen as study area to conduct wetland investigation. Block 1 locates on the inland of coastal wetland and consists mainly of high vegetation, such as mangrove forest, while block 2 locates near the sea and is full of tidal channels and low vegetation, such as reeds. Figure 1 shows the location of YRD. Figure 2 shows the ortho images of these two study sites.

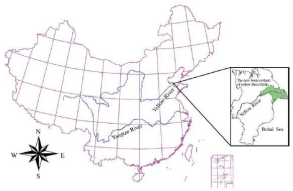

Figure 1 Location of newly created wetland of YRD (Yue, 2003)

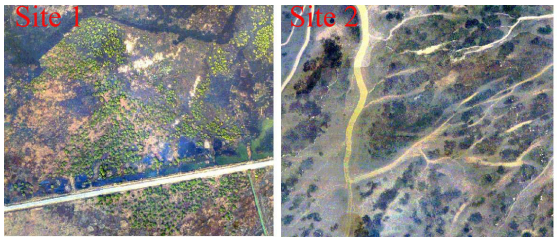

Figure 2 Ortho images of two test sites

2.2 Data acquisition

The LiDAR data employed in this study was collected in Aprial 2008 using ALS50. It can collect multi-return, and intensity can also be recorded at the same time. To cover the whole area of YRD wetland, 10 strips of data sets were collected, which covers an area of 670km^2. Each data set contains several variables: 3D coordinates, intensity, flight line, echo number and time stamp. Aerial cameras were also employed to collect

aerial images simultaneously. Table 1 detailes the specifications of sensor at the time of data acquisition.

Table 1 LiDAR data and aerial image acquisition specifications

LiDAR system	ALS50
Flying height	2400m
Field of View	62.4°
Scan rate	14.6
Pulse rate	30.2KHz
Average point distance	2.5m
Horizontal accuracy	20~30cm
Vertical accuracy	7~15cm
Aerial image resolution	1m
Bands of aerial images	Red, Green, Blue

3. METHODOLOGY

This section describes the research methods used for this study. The overall proposed methodologies are shown in Figure 3. Firstly, the datasets collected from GPS, IMU and laser scanner were integrated by GrafNav and IPAS Pro software to generate point cloud. Since error points exist, error removal algorithms were employed to remove the error points.

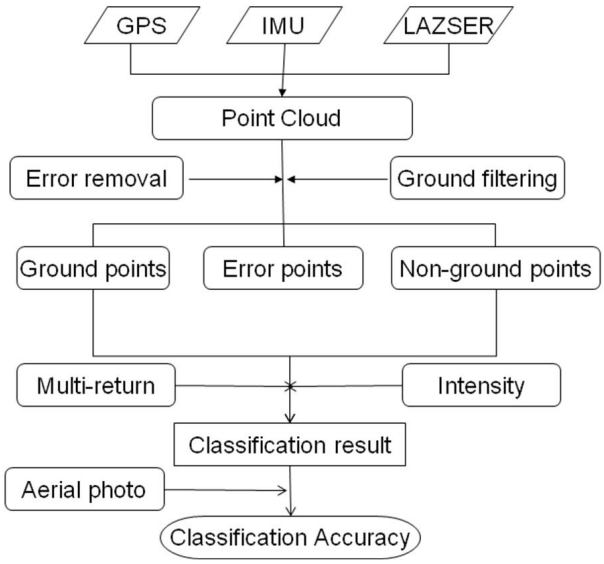

Figure 3 Proposed methodology

3.1 Error removal

Prior to undertaking spatial analysis of the LiDAR data, the main task is to classify the collected data points into different categories according to the user's requirements. The first step of this processing is to detect and to remove outliers from the point cloud. In this study, outliers are divided into two parts: low points and isolated points. Low point classification routines identify points which are significantly lower than other surrounding points. The objective is to remove those erroneous points which are clearly below the local ground. The method used compares the elevation of each point (the center point) with every other point within a given distance. If the center point is significantly lower than surrounding points, it will be classified as an outlier. The algorithm used is presented in equation (1)

$$\{D_{low}\} = \left\{ (x_p, y_p, z_p) \;\middle|\; z_{avg} - z_p > h \right\}_{(x_p, y_p) \in \omega} \quad (1)$$

where (x_p, y_p, z_p) represents a point in a window ω, z_{avg} is the average elevation in the window, h is the threshold for low point detection.

Besides low points, there are many isolated points that can be regarded as erroneous points, such as temporal objects up in the air. An isolated point classification routine is needed to classify such erroneous points. Isolated points are points which do not have many neighbors within a 3D search radius. Within a given 3D search radius, the isolated points can be identified by equation (2).

$$\{D_{iso}\} = \left\{ (x_p, y_p, z_p) \;\middle|\; N_{(x_i, y_i, z_i)} < H \right\}_{(x_i, y_i, z_i) \in R} \quad (2)$$

where (x_i, y_i, z_i) is the neighbour of point (x_p, y_p, z_p), N is the number of the neighbours in the circle, H is the threshold for the number of neighbours in a given radius R.

3.2 Ground point classification

The Adaptive Triangulated Irregular Network (ATIN) method (Axelsson, 2000) was employed in this study. The ATIN method classifies ground points by iteratively constructing a triangulated surface model. Firstly, the data set is divided into blocks whose size is determined by the largest structure in the area to make sure that all the structures (i.e. buildings and vegetation) can be filtered out. If the block size is smaller than the largest structure, the selected local low points may be on the structure rather than on the ground and will lead to misclassification. The classification starts by selecting some local low points which belong to the ground in each block. Then, an initial TIN is formed from the local lowest points. The last step is molding the model upwards by iteratively adding new points to it thereby densifying the TIN. The iterative process determines how close a new point need to be to the plane defined by currently included points in order to be accepted into the model.

Figure 4 shows the densification process of this method. The four black dots represent the classified initial ground points after the initial TIN generation. The circle represents a point that needs to be classified. For each candidate point (the circle), two parameters were calculated to judge whether it is a ground point or not. One is the angle subtended at the nearest TIN vertex. The other is the perpendicular distance from the new point to the plane. If the thresholds are met, the candidate will be added into the TIN. Otherwise, the candidate will be classified as a non-ground point which need to be further classified. The iteration process will terminate when all the candidates are processed and no new points can be added to the TIN. Based on the project data the thresholds were 10°and 1.5 m respectively.

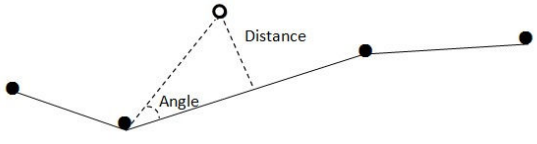

Figure 4 TIN densification process

3.3 Interpolation

After the ground points were classified, the points need to be transformed into a gridded form as this makes additional data processing more straightforward. In view of the high resolution of LiDAR data, a 3 m grid spacing was selected for the YRD data. Kriging (Stein, 1999) was used for the gridding. The remaining unclassified points belonged to vegetation or manmade features (i.e. buildings).

4. RESULTS AND DISCUSSION

Digital Surface Model (DSM) was generated with all the points came from the first return. Figure 5 shows the DSM interpolated by LiDAR point clouds with spacing of 3m. Due to the high resolution of this DSM, the topography can be explored with great detail. The road, tidal channels and vegetation can be mapped. As the geometric characteristics of LiDAR, height information of study sites can be obtained. Block 1 is dominated by high mangrove forest with average height of 9m. Block 2 is covered by reed with average height of 1.5m. By applying the classification method, LiDAR point clouds are divided into ground points and non ground points. Figure 5 shows the classified ground class. Compared with DSM, all the vegetations are removed successfully. This is difficult to achieve by using remote sensing images.

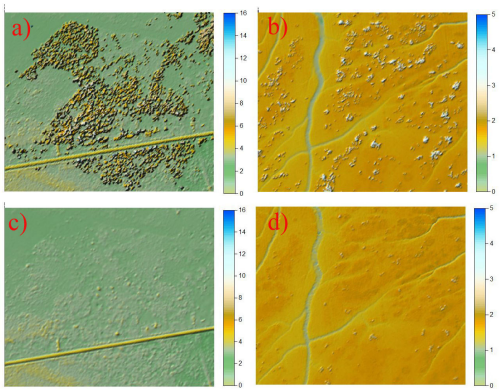

Figure 5 a) DSM of Site 1, b) DSM of Site 2,

c) DEM of Site 1, d) DEM of Site 2

4.1 Vegetation extraction

Vegetation plays an important part in protecting coastal areas from erosion, storm surge and tsunamis. Identifying the locations of costal vegetations can benefit costal wetland management. Two methods were used to extract the vegetation. One is based on the normalized DSM. As the study area is covered with only mangrove forest, and no man-made features located in. The classified non-ground points are regarded as vegetation points. It can be generated by subtracting DTM from DSM. Figure 6 a) and b) shows the normalized DSM of Site 1 and 2 which representing the vegetation distribution. The other one is based on multi-return information, which is an unique characteristic of LiDAR technology. As LiDAR pulse can penetrate the canopy and reach the ground, multi-return information can be employed to conduct vegetation extraction. All the pulses having multi-returns are regarded as vegetation points. Figure 6 c) and d) shows the vegetation location where have multi-returns. It is obviously that not all the vegetation can be penetrated by the pulse. The extracted vegetation is much less than the actual vegetation. But it can demonstrate the general distribution of the vegetation. The vegetation penetration ratio of LiDAR can be acquired by comparing the number of vegetation points from these two methods, which is 18.8% and 4.4% respectively.

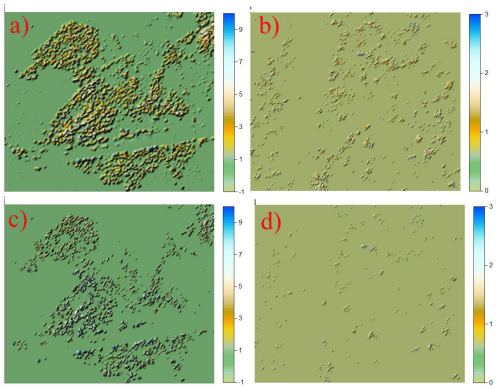

Figure 6 a) & b)Vegetation of Site 1 and Site 2 based on normalized DSM, c) & d) Vegetation of Site 1 and Site 2 based on multi return.

4.2 Statistical results

After the extraction of vegetation, we make a statistics about the extracted points. Figure 7 shows the height distribution of extracted vegetation points from only return and multi-returns.

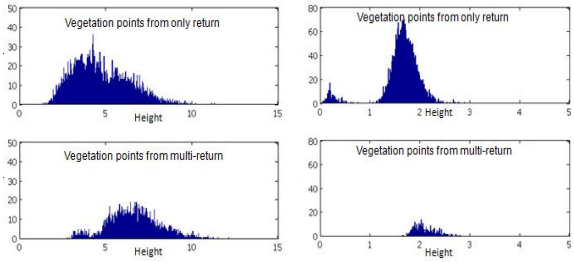

Figure 7 Height distribution of veg-points for Site 1 and Site 2.

The results demonstrate that inland wetland vegetations are large vegetation with average height of 5 m. While in wetland near the sea, low vegetations are the dominant plant. Moreover, we found that multi-return are apt to be acquired with vegetation higher than 5m in site 1. While in site 2 only small parts of vegetation were successfully extracted. The penetration ratio of LiDAR for site 1 and site 2 are 35% and 14.8% respectively.

4.3 Intensity

The intensity of the reflectance to laser beam varies on different objectives. The light LiDAR system emits is infrared which is sensitive to moisture. Figure 8 shows the intensity map of LiDAR. We can find that vegetation is difficult to discriminate from the intensity map. However, it is sensitive to targets with different moisture. The tidal channel, water region can be discriminate clearly. Here, supervised classification was employed to classify the ground into different classes with various moisture contents. Training samples were selected from aerial photo which has high resolution, and the corresponding intensity was sampled from intensity map. So, three classes were defined which were open water with intensity smaller than

30, wet ground with intensity between 30 and 150 and dry ground with intensity larger than 150.

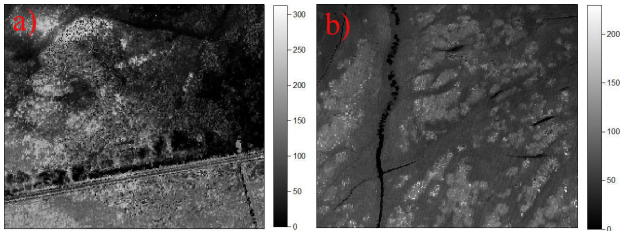

Figure 8 a) Intensity map of Site 1, b) Intensity map of Site 2

4.4 Classification results

As LiDAR can provide geometric, intensity and multi-return information, each of them has predominance in identifying a specific objective. Four classes were defined in this study area, which including open water, mudflat, dry land and vegetation. The open water has low reflectance and bare dry land has strong reflectance on intensity map. Vegetation is obviously according to the multi-return information and normalized DSM as this study area is very flat. Samples were taken from the images by manual process. Based on the extracted samples, several thresholds were defined for conducting classification. The thresholds contain the range of intensity, height and multi-return information. Figure 9 shows the classification maps for block 1 and 2. Green color represents extracted vegetation; yellow represents dry land; red represents mudflat; and blue color represents open water.

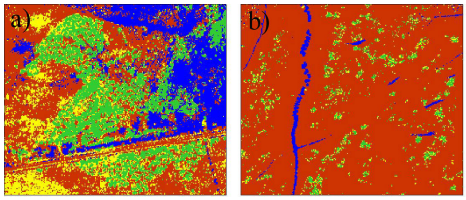

Figure 9 Classification result of Site 1 and 2

For each block, 160 points with known class are sampled as checking points from the aerial image to evaluate the accuracy of classification. For each class, 40 checking points were selected. The results show that the total classification can reach 88% and 84% for site 1 and site 2 separately. In vegetation class, the classification accuracy is high. It can attribute to LiDAR's geometric characteristics.

Table 1 Accuracy result of Site 1

Site 1		Actual classes			
		Water	Mudflat	Dry ground	Vegetation
Predicted classes	Water	37	6	2	0
	Mudflat	3	30	4	0
	Dry ground	0	4	34	0
	Vegetation	0	0	0	40

Table 2 Accuracy result of Site 2

Site 2		Actual classes			
		Water	Mudflat	Dry ground	Vegetation
Predicted classes	Water	35	4	1	0
	Mudflat	5	28	5	1
	Dry ground	0	8	34	1
	Vegetation	0	0	0	38

5. CONCLUSION

LiDAR technology emerged as a robust tool for many applications. It offers a potential alternative to field surveying and remote sensing technology. This paper chose the Yellow River Delta, which has typical coastal wetland in China, as a study area and employs LiDAR as a robust method to conduct the wetland investigation. The experiment result reveals that 1) LiDAR has prominent ability in detailed and precise mapping compared with traditional technology. 2) The penetration characteristic allows the extraction of the underneath terrain details and the vegetation. The multi-return can also be used for vegetation extraction, but it just demonstrates the distribution of vegetation, not all the vegetation can be detected. 3) Intensity data is susceptible to target with various moisture content. Open water and bare ground can be detected from intensity map. 4) The combination of these attributes makes contribution to wetland classification. The classification result can reach 88% and 84% respectively.

6. Reference

Axelsson, P., 2000. DEM generation from LASER scanner data using adaptive TIN models. In International Archives of Photogrammetry and Remote Sensing, Vol. XXXIII, Part B4, 111–118.

Carlson, T.N., Ripley, D.A., 1997. On the relationship between NDVI, fractional vegetation cover, and leaf area index. Remote Sensing of Environment 62, 241-252.

Li, X.T., Huang, S.F., Li, J.R., Xu, M., 2007. The study of wetlands change in the Yellow River Delta based on RS and GIS. Geoscience and Remote Sensing Symposium, IGARSS 2007. IEEE International, 4607-4610.

Turner, D.P., Cohen, W.B., Kennedy, R.E., Fassnacht, K.S., Briggs, J.M., 1999. Relationship between leaf area index and Landsat TM spectral vegetation indices across three temperate zone sites. Remote Sensing of Environment, 70, 52-68.

Waring, R.H., Way, J., Hunt, E.R., Morrissey, L., Ranson, K.J., Weishampel, J.F., Oren, R., Franklin S.E., 1995. Imaging radar for ecosystem studies. BioScience, 45, 715-723.

Xu, X.G., Liu, W.Z., Qi, H.Q., 2003. Wetland landscape changes and natural environmental protection in the Yellow River estuary region. International Conference on Estuaries and Coasts, Nov. 9-11, 2003, Hangzhou China, 693-699.

Yue. X.T., J.Y. Liu, S.E., Jørgensen, Q.H., Ye (2003). Landscape change detection of the newly created wetland in Yellow River Delta. Ecological Modelling. 164: 21-31.